Desalination and Water Treatment
www.deswater.com
doi: 10.1080/19443994.2015.1038113

57 (2016) 10012–10019
May

Taylor & Francis
Taylor & Francis Group

Comparison of hollow fiber membranes in direct contact and air gap membrane distillation (MD)

Hyeongrak Cho[a], Yong-Jun Choi[a], Sangho Lee[a,*], Jaewuk Koo[b], Taemun Huang[b]

[a]*Department of Civil and Environment Engineering, Kookmin University, Jeongneung-gil 77, Seongbuk-gu, Seoul, 136-702, Republic of Korea, Tel. +82 2 910 4529; Fax: +82 2 910 4939; email: sanghlee@kookmin.ac.kr (S. Lee)*
[b]*Korea Institute of Civil Engineering and Building Technology, 283 Goyangade-ro, Ilsanseo-gu, Goyang-si, Gyeonggi-do, 411-712, Republic of Korea*

Received 15 January 2015; Accepted 30 March 2015

ABSTRACT

Hollow fiber microporous membranes was used for seawater desalination in direct contact membrane distillation (DCMD) and air gap membrane distillation (AGMD) configurations. The efficiencies of hollow fiber membranes with different membrane materials and pore size were compared in a laboratory-scale DCMD system. The water flux and salt rejection were shown to be different depending on the membrane properties. The apparent permeabilities for water vapor and NaCl ion were estimated to determine the optimum membrane distillation (MD) membranes. A novel AGMD membrane module utilizing hollow fiber membranes was designed, and its prototype was fabricated using a 3D printer. Using this AGMD module, the performance of the hollow fiber membrane was examined and compared with the results from DCMD experiments. The water flux in AGMD configuration was less than 40% of that in DCMD configuration due to high mass transfer resistance and insufficient cooling plate area. However, it holds promise for practical applications of hollow fiber MD due to the higher thermal efficiency of AGMD than that of DCMD.

Keywords: Membrane distillation; Hollow fiber; Water permeability; Air gap membrane distillation; Direct contact membrane distillation; Desalination

1. Introduction

Membrane distillation (MD) is a thermally driven desalination technology still in its early stage in terms of commercial applications [1,2]. MD produces fresh water from saline water using a hydrophobic membrane, which is only permeable to volatile compounds such as water vapor [2]. For seawater desalination, hot feed water flows into the MD membrane module, leading to a difference in vapor pressure across the hydrophobic membrane [3]. Accordingly, the purified water is collected on the permeate side. MD possesses many advantages over other desalination technologies such as reverse osmosis, multi-stage flash distillation, and multi-effect distillation: minimum use of electrical energy, operation under relatively low pressure conditions, capability of using low grade heat such as waste heat and solar heat, small footprint, and low fouling propensity [1,4,5].

*Corresponding author.

Presented at GMVP Desalination Academic Workshop, Seoul, Korea, December 9, 2014.

One of the major challenges in MD technologies is the lack of commercially available MD membranes with high performance, sufficient wetting resistance, and high thermal/mechanical resistance [1,6]. Without a suitable membrane, it is difficult to deploy MD as a cost-effective commercial technology. Accordingly, a few studies have been done to fabricate MD membranes depending on their applications. Both flat-sheet and hollow fiber MD membranes have been fabricated. However, an in-depth understanding of the relationship between MD performance and membrane properties is still required to further develop novel MD membranes.

Another challenge is the selection and optimization of module configurations [7,8]. Different MD configurations have been utilized using hydrophobic membranes. There are four major configurations including direct contact MD direct contact membrane distillation (DCMD), air gap MD air gap membrane distillation (AGMD), sweeping gas membrane distillation (SGMD), and vacuum membrane distillation (VMD) [3,8,9]. In DCMD, the hot solution (feed) is in direct contact with the hot membrane side surface so evaporation takes place at the feed membrane surface. In AGMD, stagnant air is introduced between the membrane and the condensation surface and the vapor crosses the air gap to condense over the cold surface inside the membrane cell. In SGMD, inert gas is used to sweep the vapor at the permeate membrane side to condense outside the membrane module. In VMD, a pump is used to create a vacuum in the permeate membrane side and condensation takes place outside the membrane module. Each configuration has advantages and drawbacks. For example, DCMD allows high flux of water but suffers from low thermal efficiency due to the difficulties in heat recovery. On the other hand, AGMD shows higher thermal efficiency but lower water flux than DCMD. SGMD and VMD require additional equipment such as a condenser and a pump outside of the module [10]. In addition, VMD may have problems associated with pore wetting due to hydraulic pressure difference across the membrane [11]. Currently, these four configurations are available for flat-sheet and spiral-wound membranes [12]. However, only DCMD and VMD are used for hollow fiber membranes. There are few cases that AGMD is adopted for hollow fiber MD membranes due to its difficulty in combining cooling plate with hollow fiber geometry [13,14].

In this study, the efficiencies of a few hollow fiber membranes compared in terms of water flux and rejection to provide insight into the development of novel MD membranes. Moreover, attempts have been made to design and fabricate membrane modules using hollow fiber membranes to implement hollow fiber MD for practical applications. The originality of this work lies in (1) the analysis of different hollow fiber membranes using a simple lumped-parameter approach and (2) the development of novel hollow fiber AGMD module using 3D printer and other means.

2. Materials and methods

2.1. Membranes

Five hollow fiber membranes were used for the experiments. The manufacturers of the membrane A and membrane B are confidential to proprietary limitation of liability. The membranes C and E were supplied by Econity (Gyeonggi-do, Korea). The membrane D was supplied by Membrana (Wuppertal, Germany). A laboratory-scale membrane module with the effective membrane area of 0.0125 m^2 was prepared prior to the experiments. The details on the properties of the membranes are summarized in Table 1.

2.2. Experimental setup

Two laboratory-scale MD systems, including DCMD and AGMD, were developed and used for measuring flux and rejection in MD operation, as illustrated in Fig. 1. The DCMD system (Fig. 1(a)) consists of a hollow-fiber membrane module, two recirculation pumps, a feed tank, a permeate tank, an electronic balance connected to a personal computer, temperature sensors, and two heat exchangers. The feed water was heated by the heat exchanger, and the water vapor passed through the membrane was condensed by the permeate water. The mass of water collected by the condenser was measured by the electronic balance. The AGMD system (Fig. 1(b)) is similar to the DCMD system, except that the water vapor was condensed by a cooling plate within the membrane modules. The details on the AGMD module were described in the

Table 1
Summary of the hollow fiber MD membranes

Membrane	Materials	Nominal pore size (μm)
A	Polyvinylidene fluoride	0.1
B	Polyvinylidene fluoride	0.2
C	Polyvinylidene fluoride	0.22
D	Polypropylene	0.2
E	Polyethylene	0.4

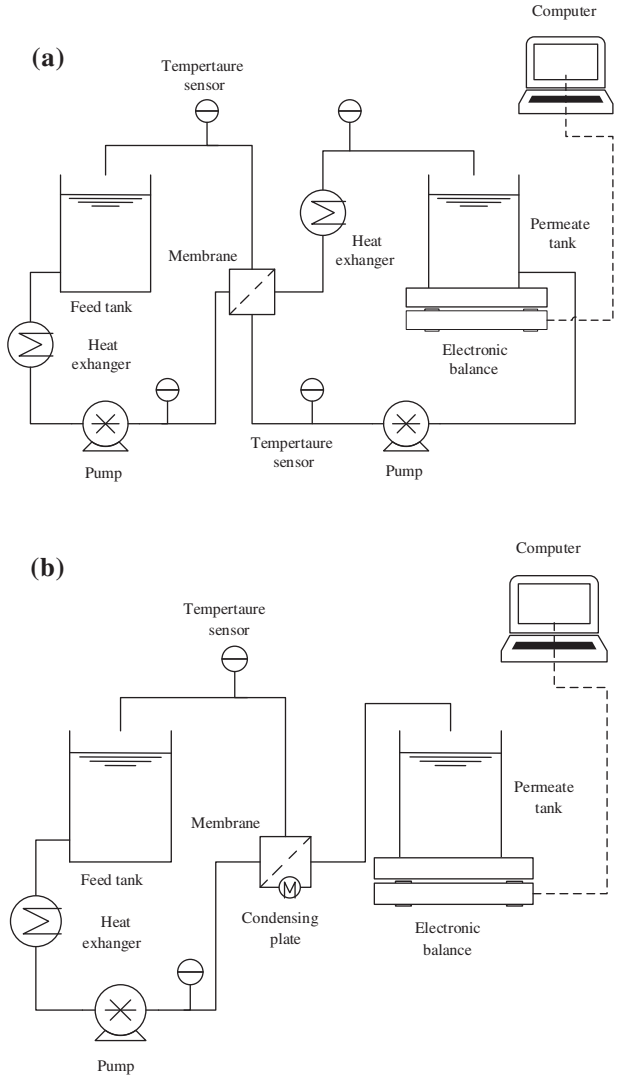

Fig. 1. Schematics of experimental setup for hollow MD: (a) direct contact MD and (b) air gap MD.

next section. Sodium chloride solution of 1,000 mg/L with the temperature of 60°C was used as the feed water.

2.3. Design of hollow fiber AGMD module

In general, AGMD configuration is not widely used for hollow fiber MD membranes. There are two problems in implementing hollow fiber AGMD: (1) difficulty in the integration of cooling plate into the membrane module and (2) recovery of heat inside the distillate and transfer to heat the new feed water. To facilitate in the design of novel hollow fiber AGMD modules, an innovative approach based on 3D modeling and 3D printing was attempted as shown in Fig. 2. First, a variety of computer models for the module were developed using the Google Sketch-up software. By examining these models, the initial screening was carried out to select several module configurations. Then, prototypes of these modules were fabricated using a 3D printer (MakerBot Replicator 2X, Brule, USA). These prototypes were initially tested to select the optimum one. Finally, the actual module was manufactured based on the final prototype. Fig. 3 illustrates the module used for hollow fiber AGMD in this study. The water vapor from the membrane is condensed by two cooling plates. The heat from the cooling plates may be transferred to the new feed water to recover latent heat. Moreover, this module enables vertical stacking to maximize the compactness of the system.

2.4. Analysis of water and salt permeability

The transport of water vapor inside the MD membrane is complex because more than two mechanisms are simultaneously involved [9,12,15]. Accordingly, it is difficult to quantify the performance of MD membranes. Here, a simple lumped-parameter approach was suggested to characterize the effeteness of MD membranes:

$$J_w = C_m (P_{feed} - P_{permeate}) \quad (1)$$

$$J_s = S_m (C_{feed} - C_{permeate}) \quad (2)$$

where J_w is the water flux (kg/m^2 h); J_s is the salt flux (kg/m^2 h); C_m is the apparent water permeability (s/m); S_m is the apparent salt permeability; P_{feed} is the water vapor pressure on the feed side; $P_{permeate}$ is the water vapor pressure on the permeate side; C_{feed} is the salt concentration on the feed side; and $C_{permeate}$ is the salt concentration on the permeate side. It should be noted that C_m and S_m are apparent values and not constant. Nevertheless, they are still useful to compare the performances of the MD membranes under same operating conditions.

The water vapor pressure can be calculated using the Antoine equation:

$$\log P = A - \frac{B}{C + T} \quad (3)$$

where T is the temperature (°C); P is the vapor pressure; and A, B, and C are constants. The vapor pressure of the saline water (P_s) is expressed as a function of the mole fraction of the solutes (x_i).

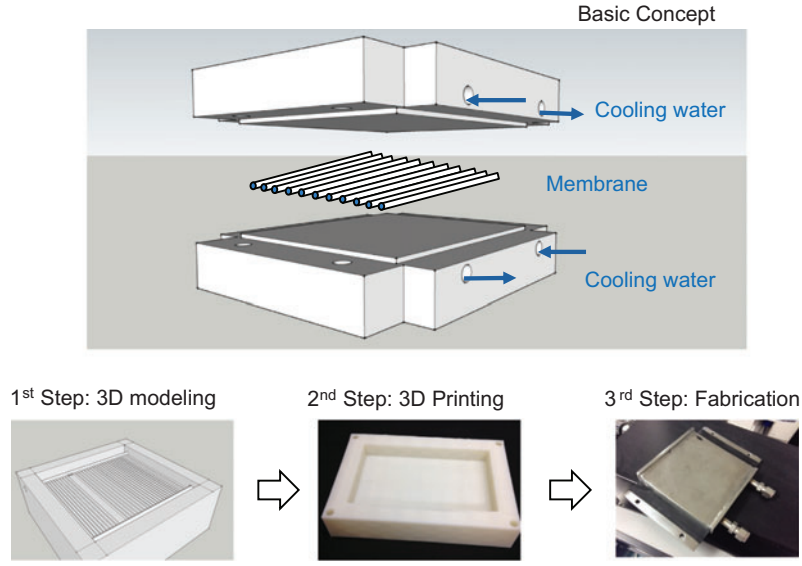

Fig. 2. Development and fabrication of air gap hollow fiber MD module.

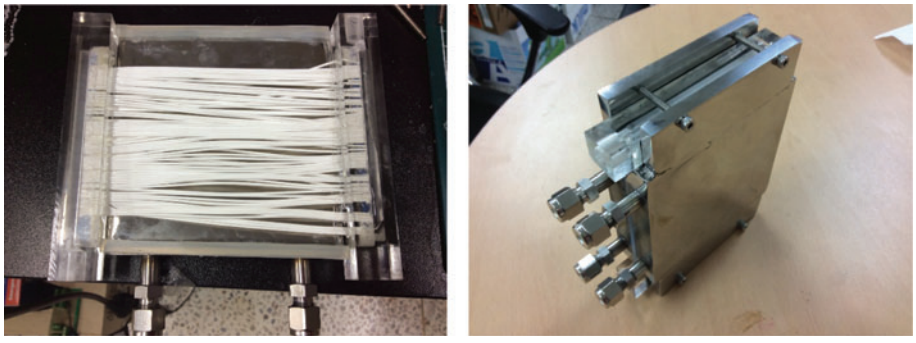

(a) (b)

Fig. 3. Membrane module for hollow fiber air gap MD: (a) membrane part and (b) housing.

$$P_s = \left(1 - 0.5(1 - x_i)^2 - 10(1 - x_i)^2\right) \cdot x_i \cdot P \quad (4)$$

Theoretically, MD membranes do not allow the salt passage. However, the salt rejection may not be 100% for most MD membranes due to salt transport by various mechanisms. Accordingly, the optimum MD membranes should have high ratio of C_m to S_m, which is suggested as a criteria for the selection of MD membranes.

2.5. Scanning electron microscopy

A field enhanced scanning electron microscopy (SEM) (Hitachi S-4700) was used to examine the surface of the MD membranes after dewetting. Prior to the SEM analysis, the membranes were coated by platinum.

3. Results and discussion

3.1. Comparison of different hollow fiber membranes for MD application

The membranes listed in Table 1 were compared in terms of water flux and salt rejection. The results of water flux are depicted in Fig. 4. The membranes shown in Fig. 4(a) are made of PVDF, and the membranes in Fig. 4(b) are made of PE and PP, respectively. The temperatures of the feed water and permeate were 60 and 20˚C, respectively. According to the Antoine equation (Eq. (3)), the difference in vapor

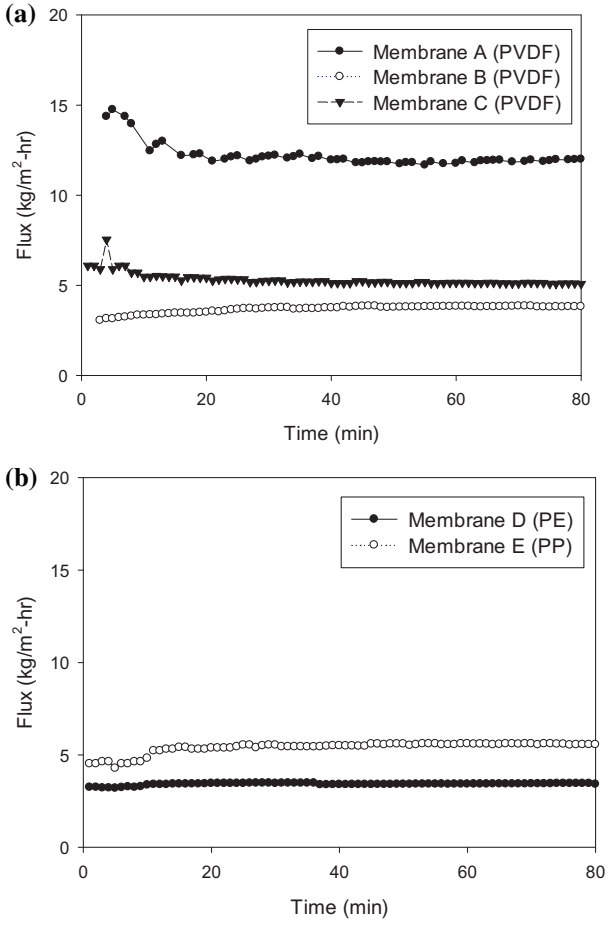

Fig. 4. Comparison of flux for different MD membranes in DCMD mode: (a) PVDF membranes and (b) PP and PE membranes.

pressure between the feed water and permeate was 0.193 bar.

The membrane A showed the highest flux (~12.2 kg/m^2 h) while the membrane D showed the lowest flux (~3.41 kg/m^2 h) under the same condition. The other membranes have the water flux ranging from 3.7 to 5.5 kg/m^2 h. It is interesting to note that the nominal pore size of the membrane is not a critical factor to determine water flux. For example, the membrane A has the pore size of 0.2 μm while the membrane D has the pore size of 0.4 μm. Unfortunately, the porosities of these membranes were not compared. However, it is evident from the results that the prediction of the water permeability from the information provided by the manufacturers is not possible. Instead, an experimental comparison is always necessary.

Fig. 5 compares the salt rejection by these hollow fiber membranes. The membranes A and B showed relatively poor rejection compared with the other three

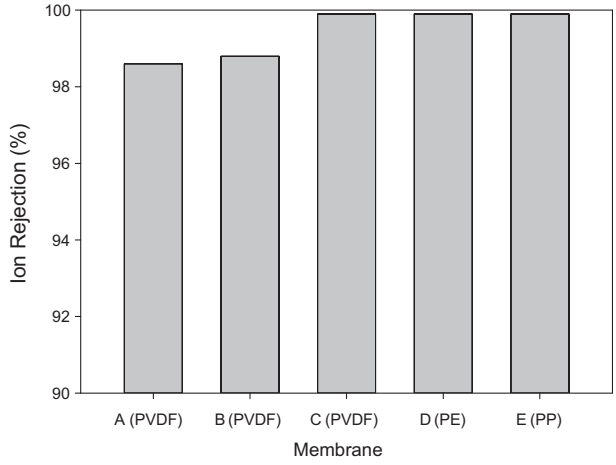

Fig. 5. Ion rejection for different MD membranes in DCMD mode.

membranes. This may be attributed to the existence of large pores that allows the passage of saline water. On the other hand, the membranes C, D, and E showed salt rejection of over 99.8%, implying that there is no large pore for water passage.

The relationship between water flux and salt rejection is demonstrated in Fig. 6, which helps to find the optimum MD membranes. The membranes with high flux and high salt rejection should be used for MD operation. For example, membrane A showed a high flux but low rejection, which may not be suitable. On the other hand, membranes C and E exhibited moderate flux and high salt rejection, which are desired for MD operation. By comparing water flux and salt

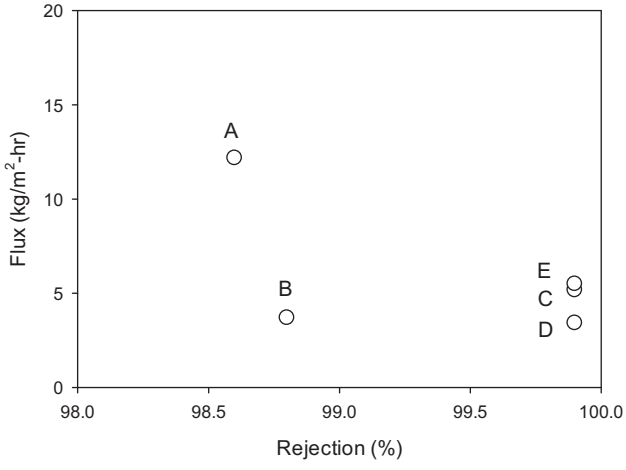

Fig. 6. Correlation between water flux and ion rejection for different MD membranes.

rejection, the MD membranes may be selected depending on their applications.

3.2. Apparent permeabilities of water and salts

Although the graphical method to determine the optimum MD membrane in Fig. 6 is helpful, a more quantitative approach is also required. Accordingly, the transport properties of the MD membranes were examined using Eqs. (1) and (2). The results are summarized in Table 2. The apparent water permeability (C_m) was the highest for the membrane A and the lowest for the membrane E. On the other hand, the salt permeability (S_m) was the highest for membrane A and the highest for the membrane E. In general, as the water permeability increases, the salt permeability increases. The exception is the membrane B, which has low water permeability and high salt permeability.

The ratio of C_m to S_m (C_m/S_m), which indicates the selectivity of water to salt, was also shown in Table 2. Since the MD membrane should have high selectivity to water transport, the higher value for C_m/S_m is better. As listed in Table 2, the membranes C and D showed the highest C_m/S_m values, suggesting that these membranes are more suitable for MD operation than the other membranes. Accordingly, the experiments in the remaining part of this study were done using the membrane C.

Table 2
Apparent permeability of water vapor for MD membranes

Membrane	C_m ($\times 10^{-8}$ s/m)	S_m ($\times 10^{-6}$ m/s)	C_m/S_m ($\times 10^{-2}$ s^2/m^2)
A	17.52	47.3	0.37
B	5.30	12.2	0.43
C	7.43	1.43	5.19
D	7.89	1.52	5.19
E	4.91	0.95	5.17

3.3. Apparent permeabilities of water and salts

Fig. 7 shows the SEM images of the membranes used in this study. Although the nominal pore sizes were similar, the actual structures were quite different. This is attributed to the difference in membrane preparation techniques. Again, there seems to be no clear correlation between the membrane pore

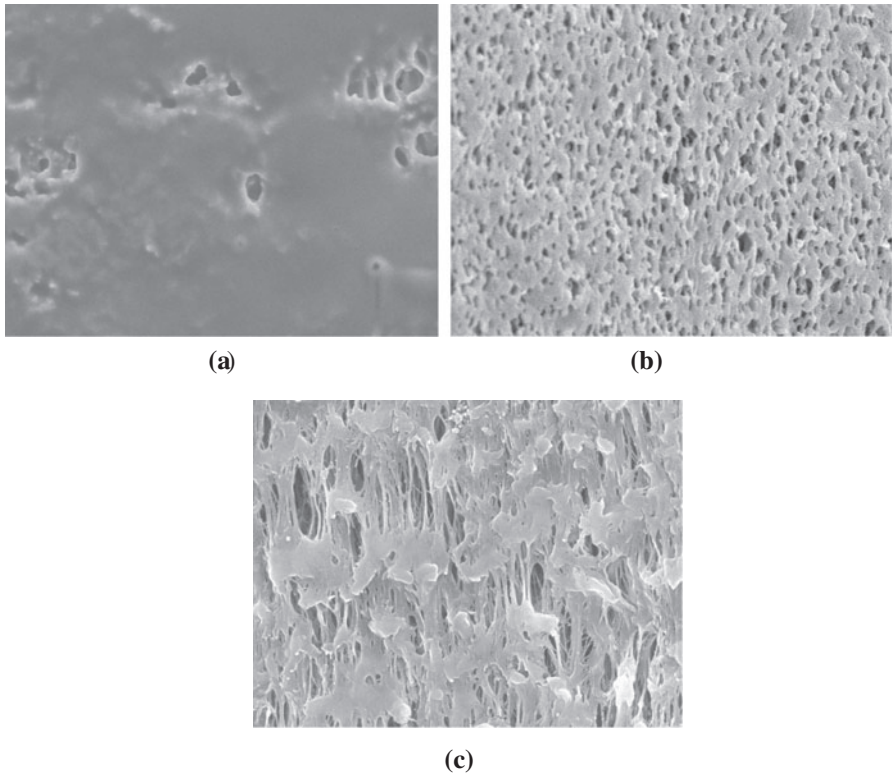

Fig. 7. SEM images for MD membranes: (a) membrane A, (b) membrane B, and (c) membrane C.

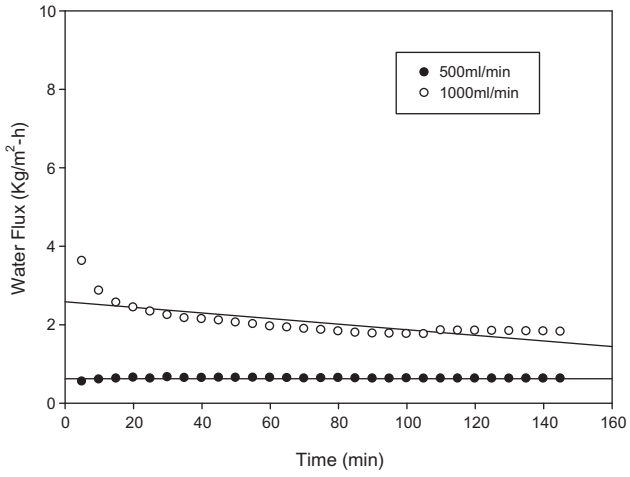

Fig. 8. Dependence of water flux through the MD membrane C in AGMD mode: (a) Q_{feed} = 500 mL/min and (b) Q_{feed} = 1,000 mL/min.

structures and its water permeability. Since the information from SEM is limited to the surface structures, it is difficult to predict the water transport properties by analyzing this. An in-depth analysis of pore structures within the membrane is required for better understanding of the structural factors affecting water permeability in MD.

3.4. Comparison of AGMD with DCMD using hollow fiber membranes

A novel AGMD module for hollow fiber membranes was first designed and fabricated in this study. Then, the efficiency of this module was examined as a feasibility study. The results are shown in Fig. 8. The AGMD tests were done in two different feed flow rates. The water flux through the MD membrane increased with an increase in the feed flow rate. At the flow rate of 500 mL/min, the average water flux was only 0.8 kg/m^2 h while at the flow rate of 1,000 mL/min, that was 2 kg/m^2 h, which is 2.5 time higher. However, the flux at 1,000 mL/min was a little bit unstable. There may several reasons: due to high flow rate, some of the membrane pores may be partially wetted, leading to a reduction in water flux. In addition, the efficiency of the condensing plate within the module may decrease with time. Although further study is required for in-depth analysis of the flux behaviors in the AGMD module, its technological feasibility could be confirmed by this proof-of-concept device.

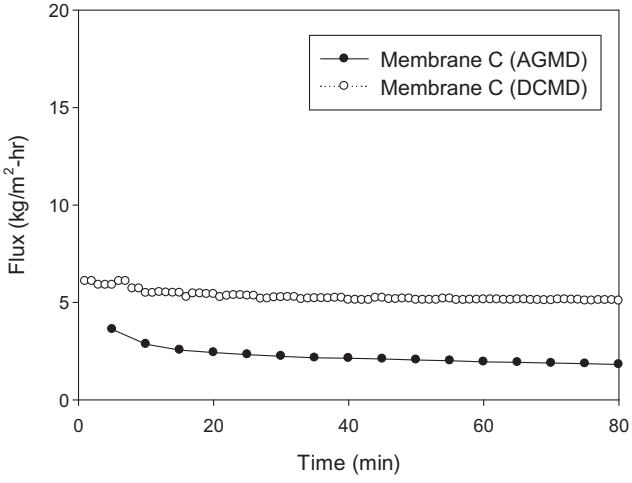

Fig. 9. Comparison of flux though the membrane C in DCMD and AGMD modes.

Fig. 9 compares the water flux in AGMD with that in DCMD under same feed water conditions. The temperature of the cooling plate was set to 20˚C in AGMD. The temperature of the permeate was also set to 20˚C in DCMD. The flux in DCMD was approximately 2.5 times higher than that in AGMD. As reported in the literature, the flux in DCMD should be higher than that in AGMD. This is because the air gap provides a significant vapor transport resistance. Nevertheless, AGMD is still attractive due to its higher thermal efficiency than DCMD. As membrane is the only barrier to separate the hot feed and cold permeate solutions, DCMD has high heat loss. However, AGMD has low heat loss due to the thermal insulation effect by the air gap.

4. Conclusions

In this study, MD using hollow fiber membranes in DCMD and AGMD configurations was investigated. The following conclusions were withdrawn.

(1) Hollow fiber membranes were compared in DCMD configuration in terms of water flux and salt rejection. There was no clear correlation between water flux and the pore size or membrane materials. The surface structures of the membrane do not seem to be important to determine the water permeability. Accordingly, it is suggested to carry out experimental determination of flux and rejection by MD membranes.
(2) A simple technique based on a lumped-parameter approach was suggested to select the optimum membrane by simultaneously considering water flux and salt rejection.

(3) A novel AGMD membrane module was fabricated based on computer modeling and 3D printing techniques. The feasibility of this module was experimentally confirmed.
(4) As expected, AGMD hollow fiber module showed a lower flux than DCMD hollow fiber module under similar conditions. However, considering the thermal efficiency, AGDM seems to have potential for practical implementation.

Acknowledgement

This research was supported by a grant from Ministry of Trade, Industry and Energy of Korean government (Project Number: 10048900) and also supported by a grant (code 13IFIP-B065893-01) from Industrial Facilities & Infrastructure Research Program funded by Ministry of Land, Infrastructure and Transport of Korean government.

References

[1] P. Wang, T.-S. Chung, Recent advances in membrane distillation processes: Membrane development, configuration design and application exploring, J. Membr. Sci. 474 (2015) 39–56.
[2] D.M. Warsinger, J. Swaminathan, E. Guillen-Burrieza, H.A. Arafat, J.H. Lienhard V, Scaling and fouling in membrane distillation for desalination applications: A review, Desalination 356 (2015) 294–313.
[3] E. Curcio, E. Drioli, Membrane distillation and related operations—A review, Sep. Purif. Rev. 34(1) (2005) 35–86.
[4] E. Drioli, A. Ali, F. Macedonio, Membrane distillation: Recent developments and perspectives, Desalination 356 (2015) 56–84.
[5] L.D. Tijing, Y.C. Woo, J.-S. Choi, S. Lee, S.-H. Kim, H.K. Shon, Fouling and its control in membrane distillation—A review, J. Membr. Sci. 475 (2015) 215–244.
[6] S. Goh, J. Zhang, Y. Liu, A.G. Fane, Fouling and wetting in membrane distillation (MD) and MD-bioreactor (MDBR) for wastewater reclamation, Desalination 323 (2013) 39–47.
[7] A.E. Khalifa, Water and air gap membrane distillation for water desalination—An experimental comparative study, Sep. Purif. Technol. 141 (2015) 276–284.
[8] G. Zuo, G. Guan, R. Wang, Numerical modeling and optimization of vacuum membrane distillation module for low-cost water production, Desalination 339 (2014) 1–9.
[9] M. Essalhi, M. Khayet, Chapter three—Membrane distillation (MD), in: S. Tarleton, (Ed.), Progress in Filtration and Separation, Academic Press, Oxford, 2015, pp. 61–99.
[10] M.A.E.-R. Abu-Zeid, Y. Zhang, H. Dong, L. Zhang, H.-L. Chen, L. Hou, A comprehensive review of vacuum membrane distillation technique, Desalination 356 (2015) 1–14.
[11] A. Rom, W. Wukovits, F. Anton, Development of a vacuum membrane distillation unit operation: From experimental data to a simulation model, Chem. Eng. Process. 86 (2014) 90–95.
[12] A. Criscuoli, M.C. Carnevale, E. Drioli, Modeling the performance of flat and capillary membrane modules in vacuum membrane distillation, J. Membr. Sci. 447 (2013) 369–375.
[13] R. Bahar, M.N.A. Hawlader, T.F. Ariff, Channeled coolant plate: A new method to enhance freshwater production from an air gap membrane distillation (AGMD) desalination unit, Desalination 359 (2015) 71–81.
[14] D. Singh, K.K. Sirkar, Desalination by air gap membrane distillation using a two hollow-fiber-set membrane module, J. Membr. Sci. 421–422 (2012) 172–179.
[15] I. Hitsov, T. Maere, K. De Sitter, C. Dotremont, I. Nopens, Modelling approaches in membrane distillation: A critical review, Sep. Purif. Technol. 142 (2015) 48–64.